The International Journal of Advanced Manufacturing Technology (2021) 112:1631–1639
https://doi.org/10.1007/s00170-020-06564-4

ORIGINAL ARTICLE

# Mechanical behavior and collapse mechanisms of innovative aluminum foam-based sandwich panels under three-point bending

Antonio Formisano[1] · Massimo Durante[1] · Antonio Viscusi[1] · Luigi Carrino[1]

Received: 10 September 2020 / Accepted: 21 December 2020 / Published online: 4 January 2021


## Abstract
Recent studies on innovative solutions in structural engineering fields highlight the effectiveness of closed-cell aluminum foams as traditional material/architecture core replacement in sandwich structures. This study aims to investigate the mechanical behavior and the collapse modes of innovative sandwich panels with aluminum foam as the core and stainless steel wire mesh-grid as the skins; the manufacturing process was based on the powder compact melting technique. The results of quasi-static three-point bending tests point out the beneficial effects, in terms of mechanical performance, of the reinforcement skin on the sandwiches, compared to the plain foams; this joins by their effectiveness in withstanding thermal and mechanical loads. Moreover, the investigation of the collapse mechanisms of the sandwiches with different thicknesses allows for testing the goodness-of-fit of the experimentally observed collapses with the ones predicted by the failure map from analytical models available in the literature.

**Keywords** Sandwich panels · Aluminum foam · Wire mesh-grid reinforcement · Bending behavior · Collapse modes · Failure map

## 1 Introduction

The concept of structural sandwich panels, where a lightweight core separates the stiff faces, dates back to the 1820s, but the systematic use of sandwiches as structural elements only gained acceptance in the middle of the twentieth century for aircraft systems [1]; subsequently, their employment in structural engineering applications is growing very rapidly around the world. Sandwich systems are used extensively in automotive, aerospace, marine, and industrial applications due to their relatively high structural efficiency, proved by high strength-to-weight and stiffness-to-weight ratios, and thermal insulation and acoustic damping properties [2]. Their many strong points, the development of new materials, and the need for high-performance and low-weight structures insure that sandwich constructions will continue to be in demand [3].

In recent years, metal foams proved to be a potential solution for enhanced sandwich cores, since they overcome some limitations typical of very common core architectures and materials for engineering applications, like honeycomb and polymer foams [4]. Specifically, the first ones are characterized by relatively high strength but show problems of deterioration over time and anisotropy [5]. The second ones, mainly used for the construction of building panels, have the advantage of being lightweight and insulating by a thermal point of view but deteriorate slightly above room temperature [6].

Metal foams are cellular structures consisting of solid metal, containing a large volume fraction of gas-filled pores, with peculiar properties that arise from the combination of their metal nature and their morphology [7]. Different metals can be processed for obtaining foams and, among them, the aluminum alloys are very useful to realize cell-structured systems characterized by relatively high properties, such as low specific weight coupled with high energy absorption capacity, high specific stiffness, and reduced thermal and electrical conductivity [8].

There are several ways to produce aluminum foams [9]; a very promising method based on the gas-releasing particle decomposition in semi-solids is known as powder compact melting technique, where an aluminum alloy and a blowing agent in the form of fine particles were mixed and then compacted to obtain the so-called foamable solid precursor [10, 11]. Heating the precursor to a little above the melting

✉ Antonio Viscusi
antonio.viscusi@unina.it

1 Department of Chemical, Materials and Production Engineering, University of Naples Federico II, Piazzale Tecchio 80, 80125 Naples, Italy

temperature of the alloy leads the compacted metal matrix in a semi-liquid viscous state; the foaming agent, distributed homogeneously within the metal matrix, decomposes and releases hydrogen, which blows bubbles in the soft alloy. Under these conditions, the released gas forces the melting precursor material to expand, modeling a highly porous structure taking the shape of the mold [12].

Generally, aluminum foam–based sandwich panels have facing of composite materials (in particular, based on carbon fibers) or lightweight metal alloys, due to their low density and high specific strength and stiffness. Carbon fiber/aluminum foam sandwich structures, although used in several engineering fields [13, 14], show poor interfacial toughness and poor residual properties after impact or crack initiation [15]. In addition, their use at high temperatures is restricted by the glass transition temperature of the matrices [16]. While ensuring good performances at high temperatures compared to the composite materials [17], also the lightweight metal alloys however show problems related to the core/skin joining methods. In fact, sandwiches obtained through adhesion cannot be used under high temperatures [18], while the brazing can cause an interfacial reaction and produce a brittle intermetallic compound [19].

Therefore, this research work aims to investigate the mechanical behavior and the collapse mechanisms of innovative metal foam–based sandwich panels, capable of combining lightness and thermomechanical properties, under flexural working conditions, through an experimental approach; moreover, the possibility of developing failure maps from analytical models available in the literature, so providing a helpful tool to predict the collapse modes of such structures, is analyzed.

For this purpose, sandwiches with three different thicknesses were manufactured by an innovative and time-effective in-mold foaming process, based on the powder compact melting technique [20]. More in detail, an essential role for the success of the sandwich structures is played by the core/skin interface that must be able to transfer loads between faces and cores [21], and the solution employed in this work allows for avoiding the core/skin joining step; in so doing, the process can be preferable to two-step (foaming and core/skin joining) methods like the hot-rolling [22] and the friction stir welding [23].

A stainless steel mesh-grid, with high corrosion and heat resistance, was used as reinforcement skins. Its size was chosen to withstand thermal (heating) and mechanical (foam expansion) loads, ensuring a satisfying core/skin coupling and reinforcing the foam panels [24]. In fact, this product was already used as die [25, 26] for the manufacture of aluminum foam components with complex shape, since the precursor can be foamed by optical heating (because the light passes through the mesh), but not as reinforcement. Actually, it was chosen with smaller diameter of the wires and clearer opening, to result in an effective solution to make the peel off of the mesh-grid from the foam easier.

Quasi-static three-point bending tests were performed on both sandwiches and plain foam panels, in order to quantify the improvement in load-carrying capacity as effect of the reinforcement skin. Moreover, great attention was paid to the failure modes of the investigated systems as well as the collapse mechanisms governing the sandwich constructions, by varying the dimensions of the panels and the load conditions. In particular, the possibility of using the failure maps obtained by the analytical models proposed by Ashby et al. [12] was explored.

## 2 Theory and methodology

This section concerns the materials, the foaming process, and the mechanical tests for the manufacture and the characterization of the foam-based sandwiches. Furthermore, it describes the theoretical background at the basis of the failure maps according to Ashby et al. [12] and the approach followed in this work to adapt the theoretical models to the proposed sandwich structures.

### 2.1 Materials and manufacturing process

The source constituents used for the manufacture of the sandwich panels were:

- A T-316 0/90 stainless steel wire mesh-grid as skins
- A foamable solid precursor supplied by Alulight, made by a powder mix of AlSi10 as aluminum alloy and titanium hydride (0.8 wt.%) as foaming agent, for the core

The main characteristics of the constituents and the nominal dimensions of the sandwich panels are reported in Fig. 1; the sandwich thickness is indicated as $2t+c$, where $t$ and $c$ are the face and core thicknesses. The face thickness ($t$) was considered constant and equal to 1.4 mm, namely, the thickness of the mesh-grid.

Each sandwich panel was produced by the precursor in such quantity (from 80 to 160 g) as to have a nominal density of the aluminum foam equal to $0.6 \cdot 10^{-3}$ g/mm$^3$; this value translated into a relative density of about 0.23, falling into the typical range of commercial metal foams (that is 0.1 ÷ 0.3 [12]).

Besides, also panels of plain foam with the same relative density of the sandwich cores were manufactured (a thickness of 12 mm was considered), to compare them to the sandwiches and to estimate the enhancement of bending properties when using the reinforcement.

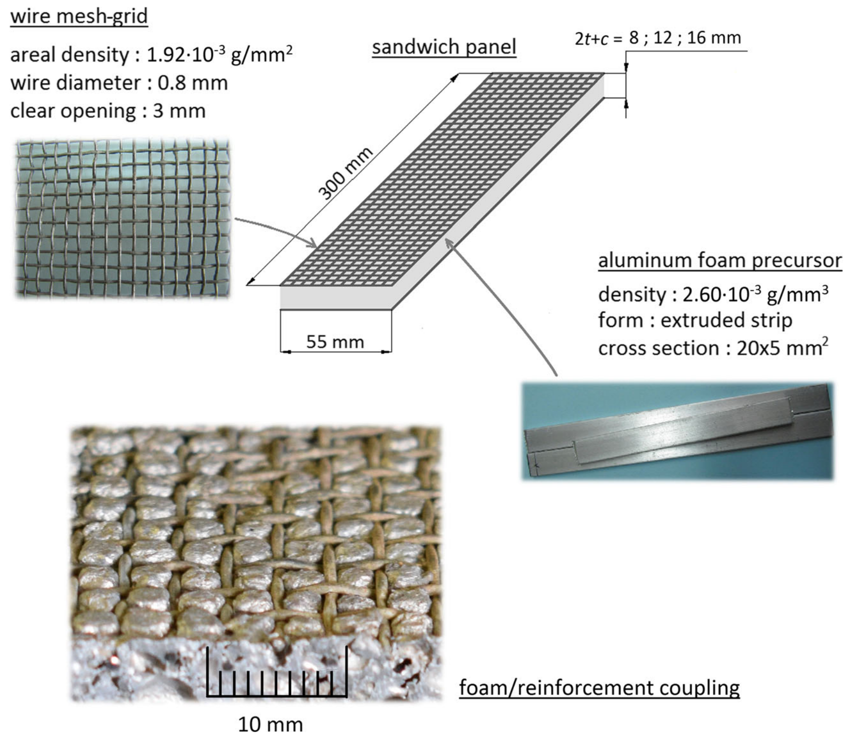


**Fig. 1** Main characteristics of the source constituents, nominal dimensions of the sandwich panels, and particular of the foam/reinforcement coupling

The main mechanical properties of the aluminum foam and the mesh-grid are summarized in a previous experimental/numerical authors' work [24].

A schematic diagram of the manufacturing sequence and the process parameters are reported in Fig. 2. Two rectangles of wire mesh-grid with the dimensions of the skins, alternate to chops of precursor, were placed inside a stainless steel thin-walled split mold (Fig. 2, step I; further details about the mold in [20]). This last was sealed, setting the desired distance between its inner faces, in order to obtain the designed sandwich

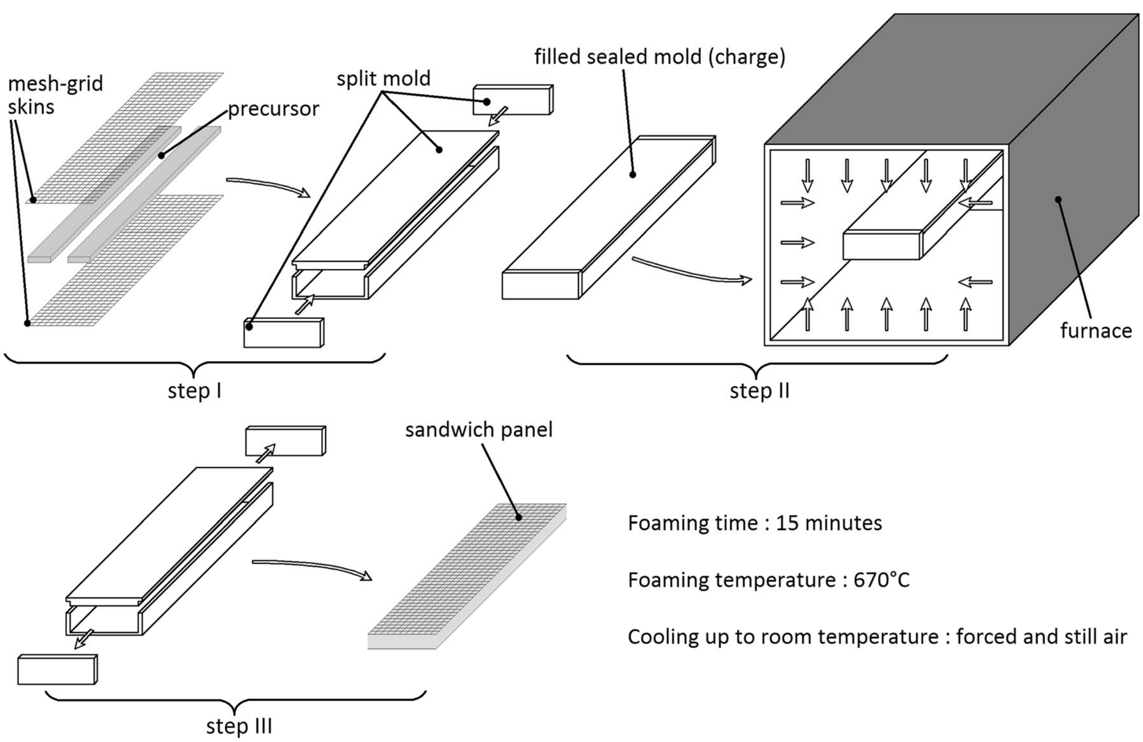


**Fig. 2** Manufacturing sequence and process parameters for the sandwich panels

thickness ($2t + c = 8$; 12; 16 mm). The charge was heated to a little above the melting temperature of the alloy into a N200/G Nabertherm chamber furnace with wire heating; the decomposition of the foaming agent created voids with a high internal pressure that expanded by semi-solid flow until the swelled alloy filled the mold correctly (Fig. 2, step II). Afterwards, the charge was taken out from the furnace and cooled (first in forced and then in still air) up to the room temperature and, then, the sandwiches were extracted from the split mold (Fig. 2, step III).

A previous authors' work [20] highlighted that the chosen process parameters guarantee complete filling of the mold and correct foaming (similar bending properties of commercial Alulight foam panels) and avoid undesirable phenomena like growth, coalescence, and collapse of the gas bubbles [27]; in addition, ad hoc shear adhesion tests ensured that they allow leading an efficient foam/mesh-grid mechanical coupling (see the particular in Fig. 1), with a satisfying load transfer from the matrix to the reinforcement and without incurring in the skin slip.

## 2.2 Mechanical tests

Quasi-static three-point bending tests were carried out through an MTS Alliance RT/50 testing machine, measuring the load with a 50 kN load cell. A crosshead speed of 4 mm/min was set; the radiuses of the supports and the loading nose, namely, the cylindrical indenter, were 5 mm.

Sandwiches with the three different thickness values were tested to estimate the capacity of enhancing the bending strength of the foam panels through the wire mesh-grid reinforcement (the comparison was made between plain foam and sandwich panels with a thickness of 12 mm) and, mainly, to investigate the collapse modes for different ($c/l$, $t/c$) coordinates of the failure map. The tests were performed by varying the span length, $l$, from 20 to 220 mm (compliance with the limits imposed by the longitudinal dimensions of the specimens and the dimensions of the fixtures) in order to generate load conditions that can cause the different sandwich collapses. The bending test plan is reported in Table 1. Three specimens were tested for each test typology for the repeatability of the experimental results.

## 2.3 Failure maps

Ashby et al. [12] associated the collapse of a sandwich structure to the lowest collapse load among the ones related to the working conditions at which the structure is subjected. Relatively to three-point bending addressed in this work: Fig. 3 sums up the operative collapse modes that are face yielding, core shear, and indentation, and the authors mentioned above reported a formula of the collapse load for each case ($F_{FY}$, $F_{CS}$, and $F_I$, respectively).

**Table 1** Bending test plan

| Panel thickness, $2t + c$ (mm) | $t/c$ (−) | Span length, $l$ (mm) | $c/l$ (−) |
|---|---|---|---|
| 8 | 0.269 | 20 | 0.26 |
| | | 25 | 0.208 |
| | | 30 | 0.173 |
| | | 40 | 0.13 |
| | | 50 | 0.104 |
| | | 140 | 0.037 |
| 12 | 0.152 | 25 | 0.368 |
| | | 40 | 0.23 |
| | | 100 | 0.092 |
| | | 200 | 0.046 |
| 16 | 0.106 | 50 | 0.264 |
| | | 100 | 0.132 |
| | | 220 | 0.06 |

The collapse mechanisms can be represented on a diagram (the failure map) with the non-dimensional axes $c/l$ and $t/c$. Non-dimensional curves, reported in Fig. 3 and identifying the collapse domains, can be drawn for determined values of $a/l$ and $\sigma_{Y,c}/\sigma_{Y,f}$, where $a$ represents the dimension of a flat-bottomed indenter that transfers the load (flat surfaces of the loading nose and the supports) and $\sigma_{Y,c}$ and $\sigma_{Y,f}$ the yield strength of core and faces, respectively. To completion of the features reported in Fig. 3 $\tau_{Y,c}$ represents the shear yield strength for the foam core and $b$ the width of the sandwiches.

It is worth noting that for the core shear collapse mode, two competing collapse mechanisms can be identified for a sandwich panel in three-point bending test. The former, generally labeled as mode A, comprises plastic hinge formation at mid-span of the sample, with shear yielding of the core; the latter, referred as mode B, consists of plastic hinge formation both at mid-span and at the outer supports of sandwich panel. The core shear collapse mode taking place was proved to be strictly related to the length of overhang $H$ beyond the outer supports. Collapse mode A is activated for small lengths of overhang, whereas collapse mode B is activated for large overhangs. The transition length of overhang ($H_t$) is defined accordingly in Eq. 1. An illustrative simple sketch is shown in Fig. 4 to make more clearly the description of the two collapse modes involved. Further details are reported by the authors [12].

$$H_t = \frac{1}{2}\frac{t^2}{c}\frac{\sigma_{Y,f}}{\tau_{Y,c}} \qquad (1)$$

It was proved that for all the bending conditions tested in this activity, the value of $H$ exceeds $H_t$, proving that the collapse mode B only can take place; the core shear collapse load by mode B is referred as $F_{CS}$ in Fig. 3.

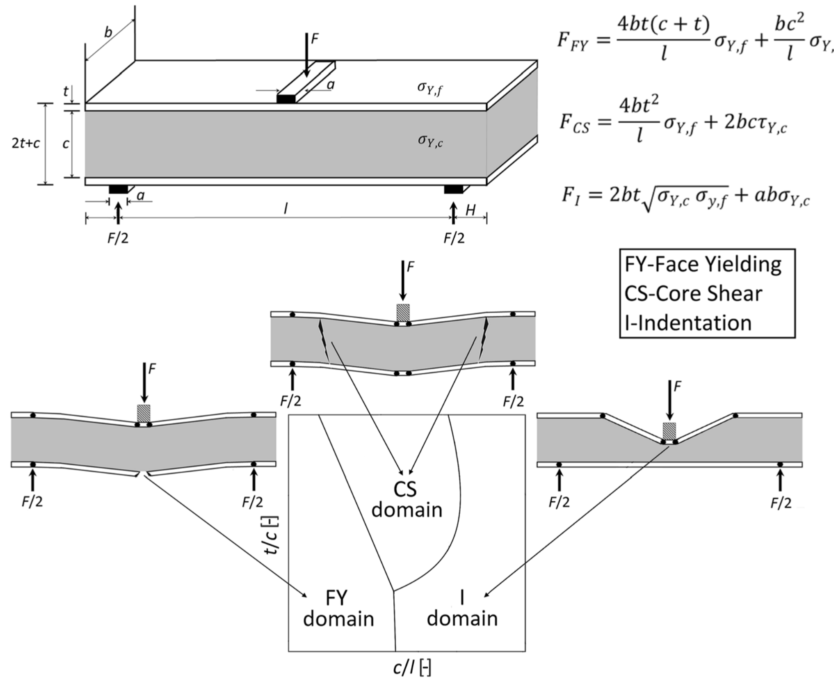


**Fig. 3** Schematization, formulae, and diagrams for the collapse mechanisms under three-point bending of sandwich panels, according to Ashby et al. [12]

Note that the formulae for the different collapse loads were derived by Ashby et al. [12] idealizing the core and the faces by rigid-ideal plastic solids, neglecting the elastic deformation; moreover, they consider homogenous metals as skins, perfectly bonded to a metal foam. Finally, this treatment was limited to the case of flat-bottomed indenters, whereas in practice, the loading of the sandwiches was by rollers.

Concerning the goodness-of-fit testing of the models proposed by Ashby et al. [12] to the experimentally observed collapses, a value of $a/l$ equal to 0.005 was set for the representation of the failure map; it represents a credible value to take into account that the sandwiches were loaded by rollers (small contact area with the sandwiches) and not by a flat-bottomed indenter. Moreover, and in order to enter the data required by the formulae in Fig. 3, compression tests on cylindrical specimens [28] and short-beam three-point bend tests on rectangular specimens of plain foam were carried out. Finally, the yield strength of the skin was evaluated according to the ASTM C393 standards, by considering a bending test that experienced face yielding ($2t + c = 12$ mm and $l = 200$ mm).

## 3 Discussion and results

The main results obtained and the discussion of them in terms of mechanical behavior and collapse modes of the sandwich structures from the three-point bending tests are reported in this section; moreover, the goodness-of-fit testing of the failure map is analyzed and extensively discussed.

It is worth nothing that each sample typology under the bending loads showed a significant repeatability of the results concerning the load-deflection behavior as well as the failure modes. Therefore, only the load-deflection curves from the tests of the exemplificative cases, namely, the curves that the authors defined as representative of the different collapse modes and the failure mechanisms involved (and not relative to the single specimen analyzed), are reported in the manuscript, for the sake of brevity.

Furthermore, the good repeatability of the results proves the effectiveness of the manufacturing method here developed as well as the beneficial effect of the reinforcement that strongly improves the mechanical behavior of aluminum foams.

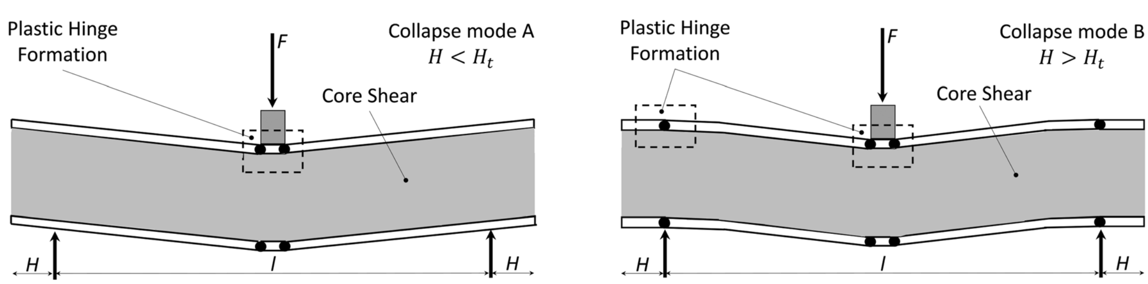


**Fig. 4** Illustrative simple sketch of core shear collapse modes A and B for sandwich panels

### 3.1 Collapse modes and mechanical behavior

Figure 5 reports a log-log failure map (with three different levels of *t*/*c* ratio, corresponding to the three different sandwich panel thicknesses) and all the different damages (see the dots labeled with the indication of the failure mode and of the span length) observed by the bending tests.

The three collapse modes, listed in Section 2.3, are found:

- Face yielding (FY)—The sandwiches affected by this failure (see Fig. 5, for $2t + c = 12$ mm and $l = 100$ mm) initially show core failure, followed by the progressive plastic deformation and necking of the wires, up to the complete sandwich failure; for this case, Fig. 6 shows the load-deflection curve (the curve for a 12-mm-thick plain foam specimen, setting a span of 100 mm, is also reported). A first fall of the load corresponds to the initial core failure, whereas the stepped shape of the descending region of the curve highlights the progressive failure of the wires. During this last phase, the failure of the foam propagates, but not dramatically, as happens for the plain foam panels. The occurrence of additional failures is even possible, so as highlighted in Fig. 5 for $2t+c = 8$ mm and $l = 140$ mm. The considerations set out above mean that the presence of the reinforcement allows a more distributed and gradual load transfer into the foam and, consequently, improved energy absorption capacity of the sandwich panels.
- Core shear (CS)—This failure is fostered by the relatively low shear strength of the aluminum foam. The main characteristics of this collapse mode (see Fig. 5, for $2t + c = 12$ mm and $l = 40$ mm) are a non-uniform and unsymmetrical bending of the sandwich and brittle through-thickness failure of the core [29], which propagates at about 30° with respect to the skins. It appears at the initial

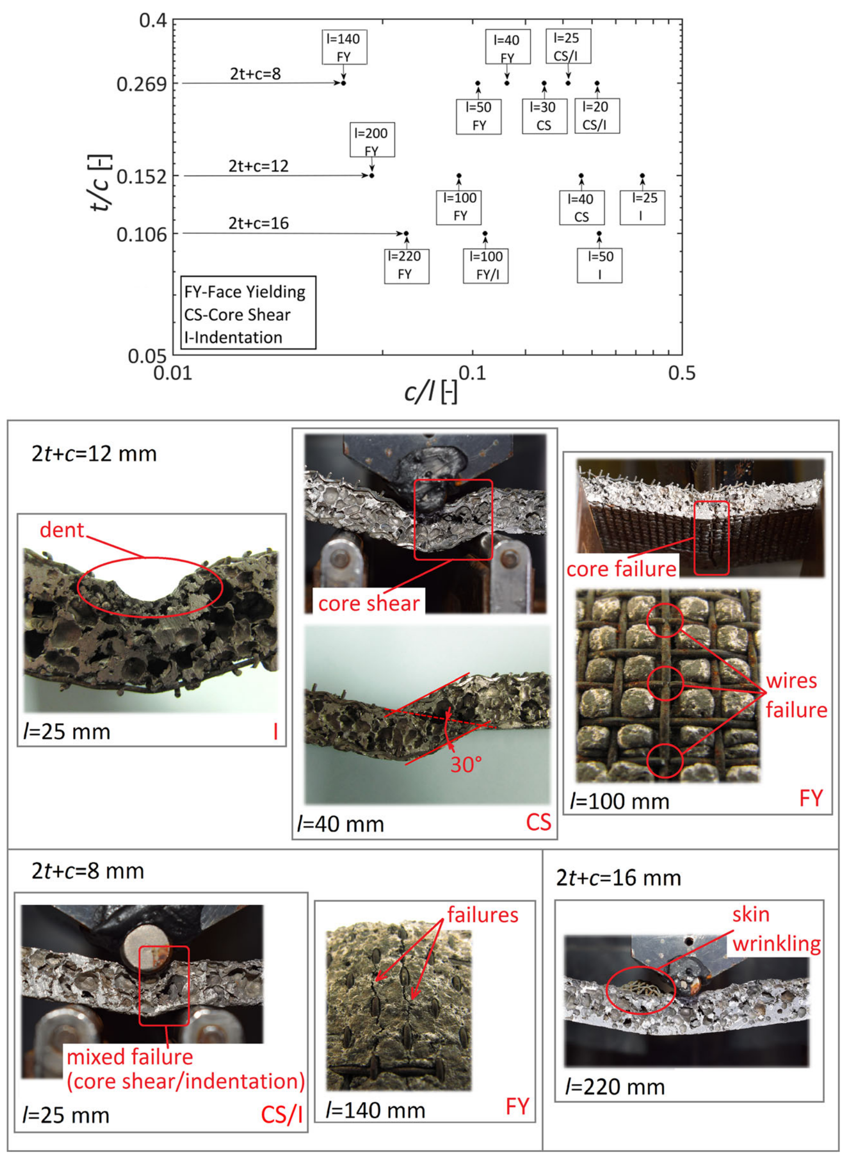


**Fig. 5** Failure map and damages observed on the sandwich panels under bending

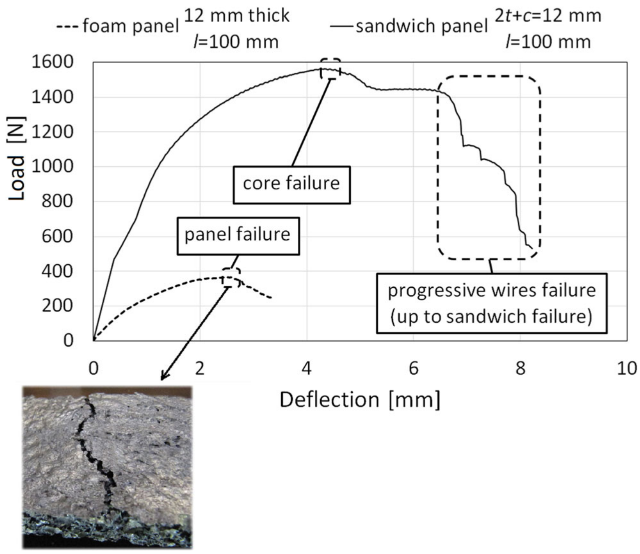


**Fig. 6** Load-deflection curves from bending tests for (12-mm thick, $l$ = 100 mm; quasi-brittle failure) plain foam panel and (2t + c = 12 mm, l = 100 mm; face yielding) sandwich panel

stage of the loading, after the initial linear elastic phase, and an abrupt drop of the bending load follows its peak. These aspects are evident in Fig. 7, where the steady-state after the drop indicates that the sandwich panel continues to resist to bending despite the extensive core crack for shear.

- Indentation (I)—This local collapse mode can occur with the increasing core thickness and the decreasing span length. Under these conditions, the deformation of the compressed upper face of the sandwich reaches a critical value; as a consequence, the deflection of the panel beneath the loading nose increases locally, forming a dent (see Fig. 5, for $2t + c = 12$ mm and $l = 25$ mm). The load-deflection curve (Fig. 7) highlights an increase of the force, due to the local densification of the foam, after which the tests were stopped without waiting for further damages.

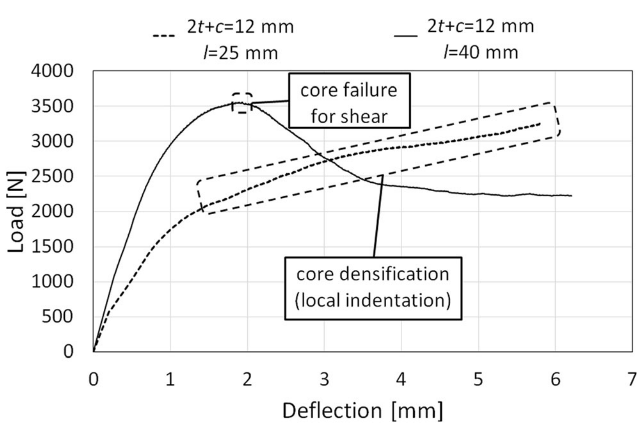


**Fig. 7** Load-deflection curves from bending tests for (2t + c = 12 mm, l = 25 mm; indentation) and (2t + c = 12 mm, l = 40 mm; core shear) sandwich panels

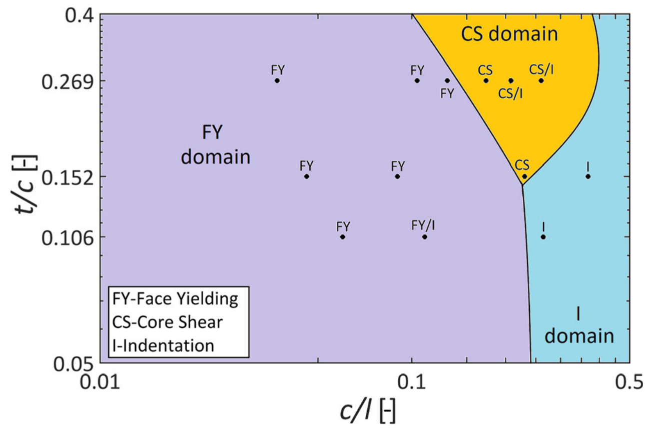


**Fig. 8** Failure map according to Ashby et al. [12] and experimental collapse modes

- For completeness, mixed collapse modes were observed; for these cases, the load-deflection curves are not reported as they show the same characteristics of the curves previously presented; however, the main features of the curves are discussed. In detail, both core shear and face yielding can be followed by incipient indentation. The first one (CS/I) was observed for the thinnest sandwich panels and with the increasing $c/l$ ratio (see, e.g., Fig. 5, for $2t + c = 8$ mm and $l = 25$ mm). In this case, the trend of the load-deflection curve is similar to what was observed for the specimens subject to the core shear failure only (see Fig. 7), presenting an increase of the load (and not a steady-state behavior) after the drop of the load, due to the beginning indentation. The second one (FY/I) interested the thickest panels, as an intermediate case between face yielding and indentation ($2t + c = 16$ mm and $l = 100$ mm). For this mixed collapse mode, no figure is reported since the damages, occurring on the two opposite sandwich faces, are similar to the already examined and shown single cases; in addition, the load-deflection curve is very similar to what was observed for the specimens subject to the face yielding failure only (see Fig. 6), with a first fall of the load that was proved to be less prominent. Finally, skin wrinkling can occur because of the combined action of the compression forces in the top facings of the sandwiches and the bonding discontinuities at the core/skin interface; this phenomenon could be observed for sufficiently thick cores and high span length [30]. An example of skin wrinkling is reported in Fig. 5, for $2t + c = 16$ mm and $l = 220$ mm; it was observed after the initial foam failure of a sandwich collapsed for face yielding. Moreover, it was proved that the load-deflection curves for both the skin wrinkling and the face yielding failures are very similar.

Figure 6 also shows a better bending behavior of the sandwiches, compared to the foam panels, while preserving the lightweight condition. In fact, net of a weight increase of about 50%, for the load conditions reported in figure the sandwich, records a 325% increase of the maximum load; furthermore, the slope of the curves in their first straight-line portion (corresponding to the elastic deformation region) and the areas under the curves suggest an increase of stiffness and energy absorption capability, respectively, for the reinforced panels.

### 3.2 Goodness-of-fit testing of the failure map

From compression tests on cylindrical specimens [28] and short-beam three-point bend tests on rectangular specimens of plain foam, a plateau stress of 9 MPa and a shear strength of 3.5 MPa were measured; they represent the values to assign to $\sigma_{Y,c}$ and $\tau_{Y,c}$, respectively.

Concerning the yield strength of the skin, a value of $\sigma_{Y,f}$ equal to 38 MPa was measured by the bending test for $2t + c =$ 12 mm and $l = 200$ mm, which experienced face yielding. This value could be predicted quite well by the weighted mean of the yield strengths of the steel wires and of the foam. In fact, for a skin thickness of 1.4 mm and by considering the areal density of the mesh-grid (see Fig. 1), its volume fraction is 0.17; by considering that the yield strength of the steel wires was equal to 195 MPa (from tensile tests on single wires, after a heat treatment similar to that during the foaming process), this procedure furnishes a value of $\sigma_{Y,f} = 40.6$ MPa.

Figure 8 reports the failure map, on which the collapse modes from the experimental campaign are labeled and represented with dots in correspondence of the ($c/l$, $t/c$) sandwich coordinates. The collapse domains are delimited by plotting the formulae of the collapse loads (see Fig. 3), in which the mechanical parameters above reported and an appropriate $a/l$ value (see Section 2.3) were implemented. The figure clearly highlights that the experimental collapses from the bending tests fall into the respective domains and, then, it is possible to affirm that the collapse prediction model proposed by Ashby et al. [12] can be used effectively for the enhanced sandwich panels described in this work.

## 4 Conclusions

The study shows the results related to the three-point bending behavior of sandwich panels, made of aluminum foam as core and a T-316 0/90 stainless steel wire mesh-grid as reinforcement, obtained by an innovative manufacturing method based on the powder compact melting technique, which allows foaming and core/skin joining in one step. The mechanical properties of the sandwiches were evaluated and compared to the ones of plain foam panel; moreover, the failure mechanisms were analyzed, through the observation of their occurrence and propagation, depending on the thickness of the sandwiches and by varying the span length.

The main results from the quasi-static three-point bending tests can be summarized as follows:

- The use of the reinforcement implies a significant improvement of the mechanical properties, compared to the plain foams, in terms of bending strength, stiffness and energy absorption capability.
- The collapse modes of the sandwiches change from face yielding to indentation with the increasing core thickness and the decreasing span length, whereas core shear occurs for high $t/c$ and $c/l$ ratios.
- Mixed collapse modes and skin wrinkling (this last fostered by the bonding discontinuities at the core/skin interface) also occur.
- The analysis of the collapse modes as a function of the dimensions of the sandwiches and of the load conditions highlights that the experimental data fit well with a consolidated prediction model based on failure maps.

## Compliance with ethical standards

#### Declarations

- No funds, grants, or other support was received.
- The authors have no relevant financial or non-financial interests to disclose.
- The authors have no conflicts of interest to declare that are relevant to the content of this article.
- All authors certify that they have no affiliations with or involvement in any organization or entity with any financial interest or non-financial interest in the subject matter or materials discussed in this manuscript.
- The authors have no financial or proprietary interests in any material discussed in this article.

## References

1. Steeves CA, Fleck NA (2004) Collapse mechanisms of sandwich beams with composite faces and a foam core, loaded in three-point bending. Part I: Analytical models and minimum weight design. Int J Mech Sci 46:561–583. https://doi.org/10.1016/j.ijmecsci.2004.04.003
2. Liew JYR, Sohel KMA (2010) Structural performance of steel-concrete-steel sandwich composite structures. Adv Struct Eng 13:453–470. https://doi.org/10.1260/1369-4332.13.3.453
3. Darzi S, Karampour H, Gilbert BP, Bailleres H (2018) Numerical study on the flexural capacity of ultra-light composite timber sandwich panels. Compos Part B Eng 155:212–224. https://doi.org/10.1016/j.compositesb.2018.08.022
4. Kee Paik J, Thayamballi AK, Sung Kim G (1999) Strength characteristics of aluminum honeycomb sandwich panels. Thin-Walled Struct 35:205–231. https://doi.org/10.1016/S0263-8231(99)00026-9

5. Khan MK, Baig T, Mirza S (2012) Experimental investigation of in-plane and out-of-plane crushing of aluminum honeycomb. Mater Sci Eng A 539:135–142. https://doi.org/10.1016/j.msea.2012.01.070
6. Carrino L, Durante M, Franchitti S, Sorrentino L (2012) Mechanical performance analysis of hybrid metal-foam/composite samples. Int J Adv Manuf Technol 60:181–190. https://doi.org/10.1007/s00170-011-3603-0
7. Kahani Khabushan J, Bazzaz Bonabi S, Moghaddasi Aghbagh F, Kahani Khabushan A (2014) A study of fabricating and compressive properties of cellular Al-Si (355.0) foam using TiH2. Mater Des. https://doi.org/10.1016/j.matdes.2013.10.022
8. Körner C, Singer RF (2000) Processing of metal foams - challenges and opportunities. Adv Eng Mater 2:159–165. https://doi.org/10.1002/(SICI)1527-2648(200004)2:4<159::AID-ADEM159>3.0.CO;2-O
9. Banhart J (2018) 4.14 Production of metal foams. In: comprehensive composite materials II. Elsevier, Amsterdam, pp 347–363
10. Rubino F, Ammendola P, Astarita A et al (2015) An innovative method to produce metal foam using cold gas dynamic spray process assisted by fluidized bed mixing of precursors. In: Key Engineering Materials
11. Formisano A, Barone A, Carrino L, et al (2018) Improvement of the mechanical properties of reinforced aluminum foam samples. In: AIP Conference Proceedings. p 100007
12. Ashby MF (2000) Metal foams : a design guide. Butterworth-Heinemann
13. Banhart J, Seeliger HW (2012) Recent trends in aluminum foam sandwich technology. In: Advanced Engineering Materials, pp 1082–1087
14. Vaidya UK, Pillay S, Bartus S, Ulven CA, Grow DT, Mathew B (2006) Impact and post-impact vibration response of protective metal foam composite sandwich plates. Mater Sci Eng A 428:59–66. https://doi.org/10.1016/j.msea.2006.04.114
15. Crupi V, Montanini R (2007) Aluminium foam sandwiches collapse modes under static and dynamic three-point bending. Int J Impact Eng 34:509–521. https://doi.org/10.1016/j.ijimpeng.2005.10.001
16. Yang P, Shams SS, Slay A, Brokate B, Elhajjar R (2015) Evaluation of temperature effects on low velocity impact damage in composite sandwich panels with polymeric foam cores. Compos Struct 129:213–223. https://doi.org/10.1016/j.compstruct.2015.03.065
17. Xi H, Tang L, Yu J, Zhang X, Xie B, Liu Y, Jiang Z, Liu Z (2015) Low velocity penetration mechanical behaviors of aluminum foam sandwich plates at elevated temperature. Int J Struct Stab Dyn:15. https://doi.org/10.1142/S0219455414500631
18. McCormack TM, Miller R, Kesler O, Gibson LJ (2001) Failure of sandwich beams with metallic foam cores. Int J Solids Struct 38:4901–4920. https://doi.org/10.1016/S0020-7683(00)00327-9
19. Song YF, Xiao LR, Zhao XJ, Zhou H, Zhang W, Guo L, Wang YH (2016) Fabrication, microstructure and shear properties of Al foam sandwich. Mater Manuf Process 31:1046–1051. https://doi.org/10.1080/10426914.2015.1037900
20. Durante M, Formisano A, Viscusi A, Carrino L (2020) An innovative manufacturing method of aluminum foam sandwiches using a mesh-grid reinforcement as mold. Int J Adv Manuf Technol 107:3039–3048. https://doi.org/10.1007/s00170-020-05244-7
21. Grünewald J, Parlevliet P, Altstädt V (2017) Manufacturing of thermoplastic composite sandwich structures: a review of literature. J Thermoplast Compos Mater 30:437–464. https://doi.org/10.1177/0892705715604681
22. Lu X, Luo H, Yang S, Wei Y, Xu J, Yao Z (2020) Two-step foaming process combined with hot-rolling in fabrication of an aluminium foam sandwich panel. Mater Lett:265. https://doi.org/10.1016/j.matlet.2020.127427
23. Peng P, Wang K, Wang W, Huang L, Qiao K, Che Q, Xi X, Zhang B, Cai J (2019) High-performance aluminium foam sandwich prepared through friction stir welding. Mater Lett 236:295–298. https://doi.org/10.1016/j.matlet.2018.10.125
24. Viscusi A, Carrino L, Durante M, Formisano A (2020) On the bending behaviour and the failure mechanisms of grid-reinforced aluminium foam cylinders by using an experimental/numerical approach. Int J Adv Manuf Technol 106:1683–1693. https://doi.org/10.1007/s00170-019-04414-6
25. Hangai Y, Amagai K, Omachi K, Tsurumi N, Utsunomiya T, Yoshikawa N (2018) Forming of aluminum foam using steel mesh as die during foaming of precursor by optical heating. Opt Laser Technol 108:496–501. https://doi.org/10.1016/j.optlastec.2018.07.016
26. Hangai Y, Nagahiro R, Ohashi M, Amagai K, Utsunomiya T, Yoshikawa N (2019) Shaping of aluminum foam during foaming of precursor using steel mesh with various opening ratios. Metals (Basel) 9:223. https://doi.org/10.3390/met9020223
27. Banhart J (2006) Metal foams: production and stability. Adv Eng Mater 8:781–794. https://doi.org/10.1002/adem.200600071
28. Formisano A, Durante M (2017) Mechanical characterization and FEM modeling of hybrid metal foam/bio-composite samples. Int Rev Model Simul 10:13687. https://doi.org/10.15866/iremos.v10i5.13687
29. Mamalis AG, Spentzas KN, Manolakos DE, Ioannidis MB, Papapostolou DP (2008) Experimental investigation of the collapse modes and the main crushing characteristics of composite sandwich panels subjected to flexural loading. Int J Crashworthiness 13:349–362. https://doi.org/10.1080/13588260801933691
30. Vonach WK (2003) Rammerstorfer FG (2003) face layer wrinkling in sandwich shells of general configuration. Comput Fluid Solid Mech. https://doi.org/10.1016/B978-008044046-0.50179-2